Microelectronics Reliability 49 (2009) 537–543

Contents lists available at ScienceDirect

Microelectronics Reliability

journal homepage: www.elsevier.com/locate/microrel

A practical investigation on nickel plated copper heat spreader with different catalytic activation processes for flip-chip ball grid array packages

Nowshad Amin [a,*], Victor Lim [a], Foong Chee Seng [b], Rozaidi Razid [c], Ibrahim Ahmad [d]

[a] Department of Electrical, Electronics and System Engineering, Faculty of Engineering, National University of Malaysia, 43600 UKM Bangi, Selangor, Malaysia
[b] Freescale Semiconductor, (M) Sdn. Bhd, No. 2, Jalan SS 8/2, Free Industrial Zone, Sungei Way, Petaling Jaya 47300, Selangor, Malaysia
[c] School of Applied Physics, National University of Malaysia, 43600 UKM Bangi, Selangor, Malaysia
[d] Department of Electronics and Communication, College of Engineering, Universiti Tenaga Nasional, Kajang 43009, Selangor, Malaysia

ARTICLE INFO

Article history:
Received 25 July 2008
Received in revised form 19 February 2009
Available online 17 April 2009

ABSTRACT

This study investigates the effects of two different catalytic activation techniques on the thermal performance of the flip-chip heat spreaders. The two activation techniques studied are thin nickel–copper strike and galvanic initiation. Thermal diffusivity and surface roughness of these heat spreaders were studied using the Nano-flash Apparatus and Infinite Focus Microscopy. High temperature storage tests were carried out to investigate the extent of intermetallic diffusion between the nickel and copper layers. The results show that heat spreaders with thin nickel–copper strike catalytic activation technique have a lower thermal diffusivity due to the low thermal conductivity of nickel–copper layer. Moreover, the nickel–copper layers grew thicker from around 0.2 μm at initial time to around 0.55 μm after high temperature storage duration of 168 h. On the other hand, heat spreaders processed using the galvanic initiation technique did not form any nickel–copper intermetallic diffusion layer. As a conclusion, the galvanic initiation technique can potentially provide better thermal performance for heat spreaders used in semiconductor packages.

1. Introduction

Thermal management is an important step in the design, manufacturing, and field service of semiconductor devices. Heat generated in the silicon during its service life has to be dissipated to ensure overall device reliability and performance for high power packages [1]. In flip-chip packages, the heat generated is dissipated via the die back to the ambient through heat sinks, as depicted in Fig. 1a [2]. Depending on customers, certain flip-chip packages require intermediate heat spreaders for better thermal performance and/or die back protection, as shown in Fig. 1b [2]. Fig. 1b shows the cross-section of a typical flip-chip ball grid array (FCBGA), in which an intermediate heat spreader made of nickel plated copper is attached on the silicon die back with thermal interface material (TIM). In turn, the larger heat sink is attached on the back of the heat spreader via second layer of TIM, as shown in Fig. 1b. Table 1 displays the typical package dimensions for FCBGA that have been marked in Fig. 1, all the dimensions will vary depending on the customer requirements.

Nickel plated copper heat spreader acts as a medium to dissipate heat from the silicon die to the larger heat sink. Copper is chosen as the material for heat spreaders in flip-chip ball grid array packages due to its high thermal conductivity [3]. A thin layer of nickel is plated to the copper to improve wear resistance and to prevent the oxidation of copper [4,5]. Nickel can be plated onto copper surfaces by either electroless plating or electrolytic plating techniques. This paper will focus on electroless nickel plating only. Electroless nickel plating technique refers to a chemical coating process that is being used to deposit nickel onto copper. This technique operates without electricity and provides a very uniform thickness over the most complicated shapes. It overcomes the major problem of non-uniform plating thickness that result from the variation in current density caused by the geometry of the plated body and its relationship to the plating anode as typically seen in electrolytic plating [5,6].

Electroless nickel deposits are generally semi-bright, but this will vary depending on bath composition and surface finish of the base material. The initial nickel deposit is self-catalyzed in the chemical reduction process, with the deposition of nickel continuing until the operator terminates the process by taking out the specimen from the bath. Provided that there is a chemically cleaned surface, metals that are spontaneously deposited with nickel when immersed in an electroless nickel plating solution, are nickel, cobalt, iron, zinc, titanium, beryllium, and palladium. Metals such as lead, cadmium, antimony, and bismuth are catalytic poisons and incapable of direct electroless nickel deposition. These metals can be electroless nickel deposited by first applying a layer of nickel electrodeposit. Plastics, ceramics, silver, copper, and

* Corresponding author. Tel.: +60 146690780; fax: +60 389216146.
E-mail address: nowshad@vlsi.eng.ukm.my (N. Amin).

0026-2714/$ - see front matter © 2009 Elsevier Ltd. All rights reserved.
doi:10.1016/j.microrel.2009.02.013

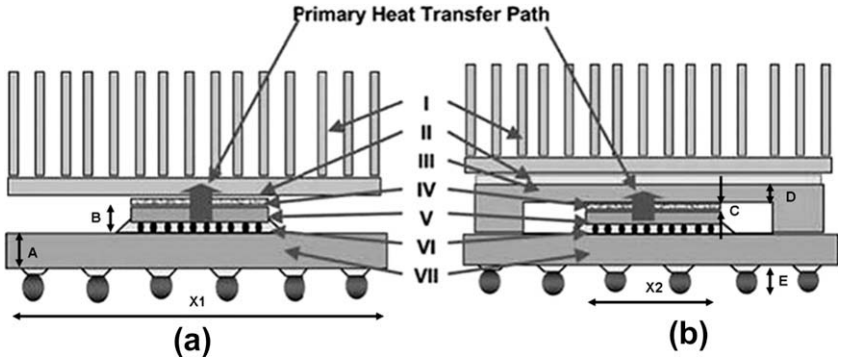

Fig. 1. Schematic illustration of thermal architectures. (a) Architecture I, typically used in laptop applications. (b) Architecture II, typically used in desktop and server applications. I – heat sink; II – TIM; III – heat spreader; IV – TIM; V – die; VI – underfill; and VII – package substrate.

copper alloys require catalytic activation such as galvanic initiation or a thin nickel electrodeposit (strike) [6].

The objective of this paper is to study the thermal performance of heat spreaders with different catalytic activation techniques. The effects of surface roughness and intermetallic growth on thermal performance of heat spreaders were also studied on freshly plated and isothermally aged specimens.

2. Experimental procedures

Two types of heat spreaders with different catalytic activation technique were used in this study. Both heat spreaders are $30 \times 30\ mm^2$ in area with 0.7 mm of thickness in the middle of the heat spreaders and plated with a thin layer of nickel. The intrinsic properties of the heat spreader are assumed to be the same but different in catalytic activation technique before plating process. Heat spreaders that contain an additional catalytic activation layer used in the present work are named as heat spreader A, while heat spreaders without additional layer are named as heat spreader B. Both heat spreaders were cross-sectioned from the side to display each layers inside the heat spreader. Elements contained inside both layers of heat spreaders were characterized using Philips XL 30 ESEM (Scanning Electron Microscope) equipped with an Oxford Instruments Inca X-sight Energy Dispersive X-ray (EDX) system. After the elements of both thin layers had been identified, thin layer formed by catalytic activation treatment process were characterized by Siemens D5000 X-ray Diffractometer (XRD) to identify the compound at the catalytic activation layer.

High temperature storage (HTS) tests for heat spreaders were performed at 150 °C for 24, 48, 96, and 168 h in Despatch LAC HTS Oven. Accelerated aging at high temperature was used to promote nickel–copper intermetallic growth. All the samples with same initial catalytic activation technique were baked under different time ranges to see the growth of catalytic activation layer. Cross-sections of heat spreader were prepared in the normal metallographic manner using Buehler Ecomet 3, by taking care not to smear the thin metal layers. In addition, the deformation of the thin metal layers due to the polishing process had to be minimized. Specimens were mounted in a low heat evolution epoxy to reduce the risk of heat-induced stress damage to the samples. After potting and curing, samples were wet-grinded with 180, 400, 800, and 2000 grit size grinding papers and then polished with 9 μm and 3 μm diamond suspension on silk cloths. Finally, samples were polished by 0.05 μm colloidal silica suspension on polyurethane cloth. Optical imaging was performed with Olympus BH3-MJL microscope to measure the thickness of each layer.

Thermal diffusivities of heat spreaders were determined using Netzsch LFA 447 Nano-flash thermal diffusivity meter after the HTS tests. The samples were cut into round shapes with diameter of 12.7 mm in order for the sample to be fitted into the test apparatus's sample holder tray. The thickness of the samples was measured by Mitutoyo Series 293 Micrometer while the density of the samples was measured by Alfa Mirage MD-300S Electronic Densimeter to get the necessary information for thermal diffusivity calculation. Samples were coated by graphite prior to thermal diffusivity test in order to enhance the absorption of laser energy and the emission of infra-red radiation to the detector. Thermal diffusivities were measured with the preset parameters of 100% optical filter, medium pulse width and 10× gain of preamp at the test apparatus.

Finally, both heat spreaders surface roughness were measured by Alicona Infinite Focus Microscope (IFM) to study the effect of different catalytic activation technique towards surface roughness of electroless nickel plating. The IFM was performed on a scanning area of 500×500 μm and the height scanned is 40 μm. For each sample, the results are presented in the 3D view of processed heat spreader surface and the section analysis showing topography of each sample. Average roughness (R_a) and root-mean-square roughness (R_q) were collected over the entire measurement.

3. Results and discussion

3.1. Identification of the catalytic activation technique

As the heat spreader for this study is made from copper and needed to be plated with nickel, therefore catalytic activation is required to deposit the initial nickel onto the surface. Deposition of the initial nickel onto the surface of the heat spreader starts the chemical reduction process. Typical catalytic activation procedures for surface treatment of metals include the application of momentary cathodic current (galvanic initiation), thin nickel strike, the application of palladium film, and the immersion of the part in reducer solution such as dimethylamineborane (DMAB) [6–9]. Catalytic activation processes for both heat spreaders were determined by EDX and XRD characterization.

Table 1
Typical FCBGA package dimensions.

Mark	Description	Dimensions (mm)
A	Substrate thickness	1.2
B	Flip-chip thickness	0.82
C	TIM thickness	0.05–0.08
D	Heat spreader thickness	0.7
E	Solder ball thickness	0.3–0.6
X1	Package area	25×25–45×45
X2	Flip-chip area	5×5–14×14

According to theory, electroless nickel plating using galvanic initiation catalytic activation process will form an additional layer of material besides electroless nickel plating layer and copper layer. However, this nickel deposit layer can be ignored because it is too thin as it is even hard to recognize under high magnification scope. Nickel, palladium, and other strike techniques also create a thin layer of deposit onto the copper substrate before electroless nickel plating process begins. The material of the thin deposit layer will depend on the material that was used to perform strike plating. Electroless nickel plating process with DMAB will only form one layer of plating deposit onto copper substrate. This deposit layer contains boron, phosphorus and nickel inside the electroless nickel plating layers.

SEM image of the cross-sectioned heat spreader A is shown in Fig. 2a. It can be found that three layers of materials exist in this heat spreader. EDX analyses performed onto the cross-section units using point scan and each layers spectrum analyses are shown in Fig. 2b–d. Nickel, phosphorus and platinum are shown in electroless nickel plating layer in EDX spectra in Fig. 2b. This layer is the electroless nickel plating layer that contains both nickel and phosphorus deposits. The followings are the cathodic reactions of electroless nickel plating:

$$H_2PO_2^- + 2H^+ + e^- \rightarrow P + 2H_2O \quad (1)$$

$$2H^+ + 2e^- \rightarrow H_2 \quad (2)$$

$$Ni_2^+ + 2e^- \rightarrow Ni \quad (3)$$

According to the above equations, hypophosphite is reduced to atomic phosphorus; hydrogen ions are reduced to hydrogen gas while nickel ion is reduced atomic nickel in the cathodic reactions [7,10]. Both the atomic phosphorus and the atomic nickel depose on the base surface forming nickel–phosphorus (Ni–P) alloy. Platinum is found in the spectrum because it was used as a coating material for better SEM image capturing, it also appear on other spectra and can be ignored for the same reasons.

The spectrum analysis in Fig. 2c shows that nickel and copper are the elements deposited on this layer. The thin layer of Ni–Cu alloy whose thickness is less than 1 micrometer produced by direct current plating from a sulphate type bath (using an aqueous citrate electrolyte containing Ni and Cu sulphates) and the alloy composition was varied by changing the deposition current density [11–15]. The followings are the cathodic reactions for nickel–copper electrodeposition:

$$Ni_2^+ + 2e^- \rightarrow Ni \quad (4)$$

$$Cu_2^+ + 2e^- \rightarrow Cu \quad (5)$$

In the cathodic reactions, nickel and copper ions in the sulphate solution change to atomic nickel and copper [9]. Both the atomic copper and the atomic nickel were deposited on the substrate's surface forming the nickel–copper thin layer. Fig. 2d shows copper is the only element found and its high intensity level suggests that this layer is the copper layer of heat spreader. Hence, nickel–copper strike was used as the catalytic activation technique for heat spreader A.

Fig. 3 shows the SEM image and the EDX spectra for heat spreader B. Only two layers of material were found inside SEM image of heat spreader B in Fig. 3a. The elements inside spectrum for electroless nickel plating layer (Fig. 3b) and copper layer (Fig. 3c) are similar with EDX spectra of heat spreader A. Electroless nickel plating layer contains nickel and phosphorous; while copper is the only material that exists in copper layer. According to the spectra, galvanic initiation catalytic activation technique was used to cata-

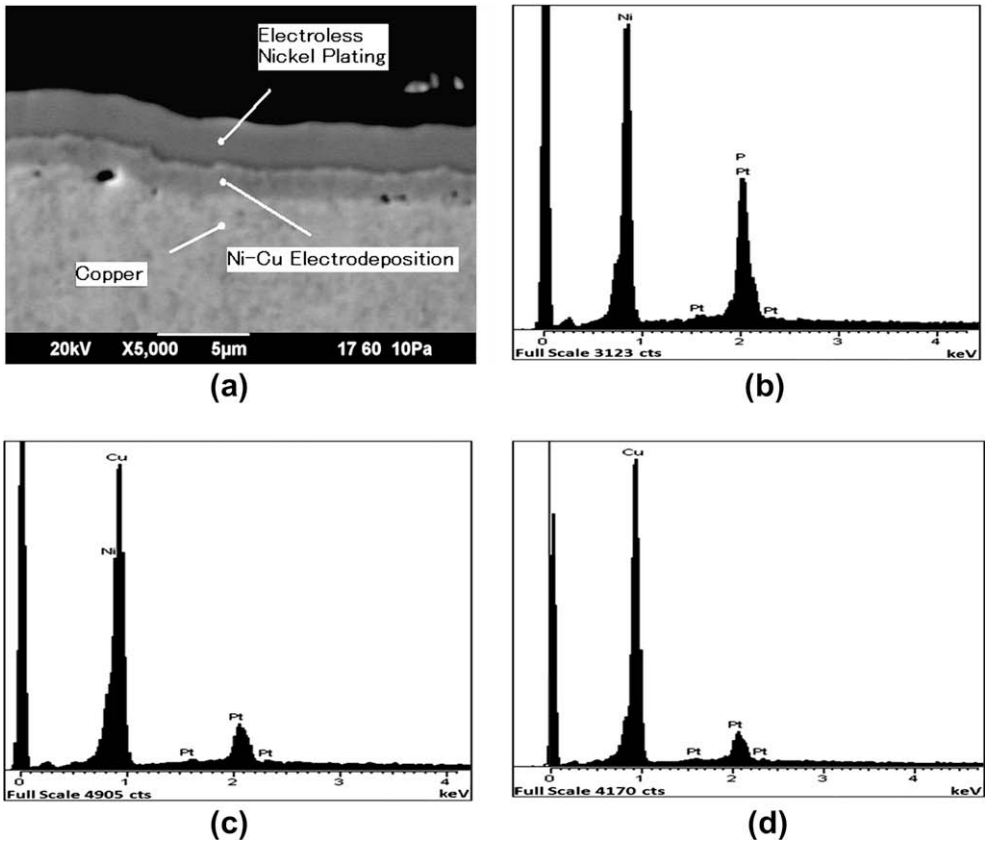

Fig. 2. SEM image and EDX spectra of heat spreader A. (a) Cross-sectional SEM image of heat spreader A; (b) EDX spectrum of electroless nickel plating layer; (c) EDX spectrum of Ni–Cu electrodeposition layer and (d) EDX spectrum of copper layer.

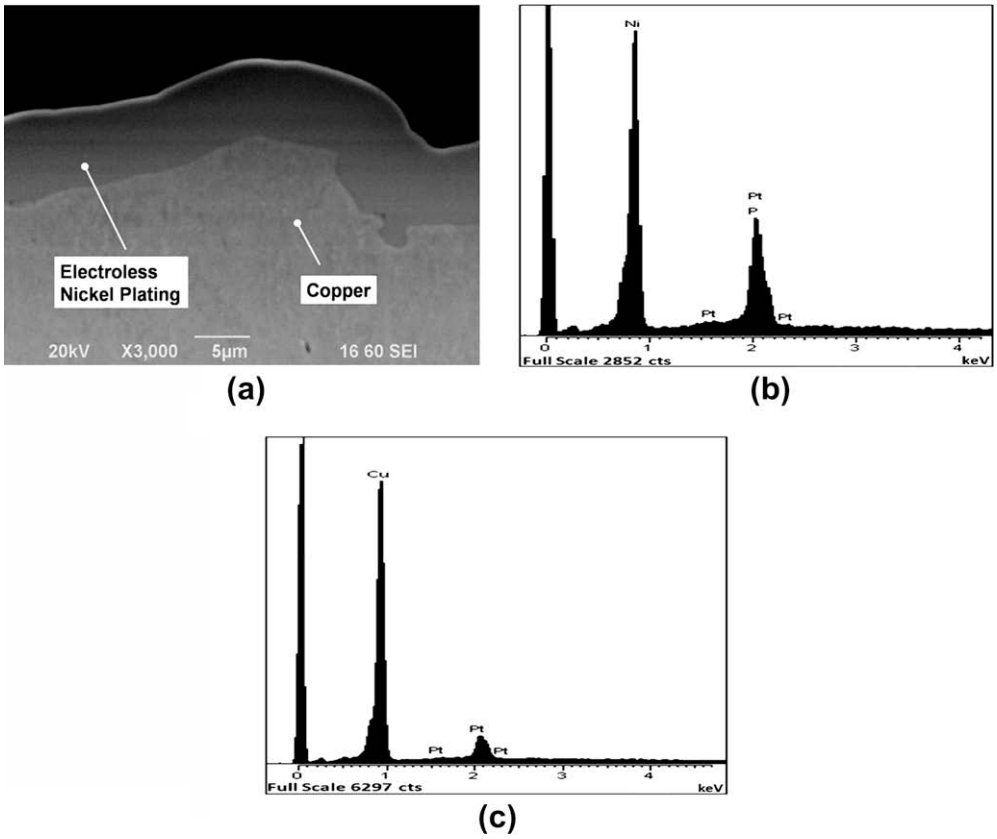

Fig. 3. SEM image and EDX spectra of heat spreader B. (a) Cross-sectional SEM image of heat spreader B; (b) EDX spectrum of electroless nickel plating layer; and (c) EDX spectrum of copper layer.

lyze the electroless nickel plating process for heat spreader B. The manufacturer uses electrolytic initiation of plating in the electroless nickel bath with a rectifier or touching the work with a piece of steel or aluminum wire. This changes the electropotential of the surface and allows plating to begin on the surface. The manufacturer uses the application of momentary cathodic current to electroplate some nickel on the surface and cut off the electricity when deposited nickel is sufficient to catalyze the electroless nickel plating process.

In normal phenomenon, nickel and copper are fully miscible and form a binary isomorphous phase diagram. With certain addition forces or under specific critical environments, two intermetallic compounds which are $Cu_{0.81}Ni_{0.19}$ and $Cu_{3.8}Ni$ may appear in the nickel–copper alloys [13,14]. XRD analysis was performed to identify the compounds that had been formed during nickel–copper strike. The XRD spectrum was edited with computer interface software DIFFRAC and EVA as shown in Fig. 4 between the range of 40° and 80°. Fig. 4 shows the XRD pattern of the copper and nickel metals while Ni–Cu bimetallic particles pattern did not exist. Pure copper shows the characteristic reflections at 43.3°, 50.4°, and 74.2° related to the (111), (220) and (220) planes. Similarly, pure Ni metal shows characteristic reflections at 44.4°, 51.8°, and 76.4°

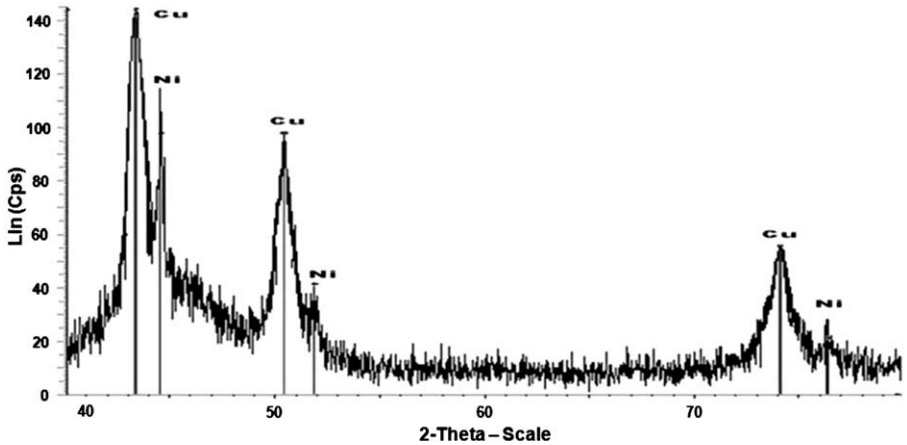

Fig. 4. XRD spectrum of Ni–Cu electrodeposition layer in heat spreader A.

corresponding to the (111), (200) and (220) planes [16–18]. This proves that thin nickel–copper strike technique did not form any intermetallic compound.

3.2. Effect of high temperature storage on intermetallic diffusion

In this section, intermetallic diffusions between each heat spreaders' layer under HTS condition were studied by normal metallographic cross-section. Fig. 5 shows the Ni–Cu electrodeposition layer for heat spreader A which has been grown under HTS condition from initial time (0 h) until 168 h. Meanwhile, Fig. 6 shows the electroless nickel plating layer was getting thinner after HTS condition. These show that intermetallic diffusion happen at Ni–Cu electrodeposition layer and electroless nickel plating layer. Diffusion of Ni–Cu electrodeposition layer actually occurred from two directions; nickel–phosphorus and copper layer. The magnitude of the diffusion coefficient D, is indicative of the rate at which atoms diffuse. Equation of diffusion coefficient is as follows:

$$D = D_0 \exp(-Q_d/RT)\ (\mathrm{m}^2/\mathrm{s}) \tag{6}$$

where D_0 is the temperature-independent pre-exponential (m^2/s), Q_d is the activation energy for diffusion (J/mol), R is the gas constant, 8.31 J/mol K and T is the absolute temperature (K). The Ni–Cu metal diffusion rate is very low which can be attributed to its lower temperature-independent pre-exponential ($D_0 = 2.7 \times 10^{-5}\ m^2/s$) and higher activation energy ($Q_d = 256$ K) if compared with other metals [3,19].

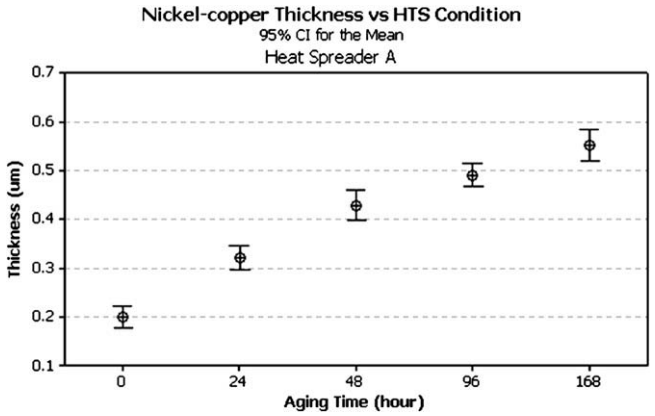

Fig. 5. Nickel–copper thickness with different time conditions in heat spreader A.

From an atomic perspective, the diffusion process is a stepwise migration of atom from lattice site to lattice site. These atomic motions can occur in two different models, namely vacancy diffusion and interstitial diffusion. Vacancy diffusion involves the interchange of an atom from a normal lattice position to an adjacent vacant lattice site or vacancy. Interstitial diffusion involves an atom that migrates from an interstitial position to a neighboring space that is empty. Interstitial diffusion happens on different size of atoms when the small sized atoms migrate through the empty space in the crystal structure of the big atoms. Both copper and nickel have face centered cubic lattice structures with almost identical lattice constants of $a_{Cu} = 0.361$ nm and $a_{Ni} = 0.352$ nm and its lattice mismatch is approximately 2.5% [11,17]. Hence, the diffusion happened at Ni–Cu electrodeposition layer is vacancy diffusion rather than interstitial atomic movement because same size atom can only diffuse in the presence of empty spaces.

Fig. 7 shows the electroless nickel plating layer thickness under different time conditions. Electroless nickel plating layer thickness does not show any trend of getting thicker or thinner in this figure. After HTS condition, heat spreader B did not show any diffusion layer formation between electroless nickel plating layer and the copper substrate. This is because the deposited atoms are arranged orderly onto the surface of copper during electroless nickel plating deposition process. There is lack of vacancy for copper atom to diffuse into the electroless nickel plating layer. Therefore, electroless nickel plating layer provides a strong wear resistance and high anti-corrosion material for today's industry. However, for the Ni–Cu electrodeposition layer in heat spreader A, nickel and copper atoms create some vacancies during deposition onto the copper surface. This facilitates copper and nickel atoms to diffuse easily inside the Ni–Cu electrodeposition layer. A very low electrodeposition current can improve the deposition quality with less vacancy created in the deposition process. But this will also affect the deposition rate to become very slow and take very long time for the deposits to reach the required thickness.

3.3. Effect of high temperature storage in thermal diffusivity

The key material property that affects transient heat conduction is the thermal diffusivity. Thermal diffusivity represents the speed heat diffuses through a material. Noted that the thermal conductivity, k represents how well a material conducts heat, and the heat capacity, ρc_p represents how much energy a material stores per unit volume. Therefore, the thermal diffusivity of a material can be viewed as the ratio of the heat conducted through the material to the heat stored per unit volume [2]. Thermal diffusivities of heat spreaders under different HTS condition were measured using

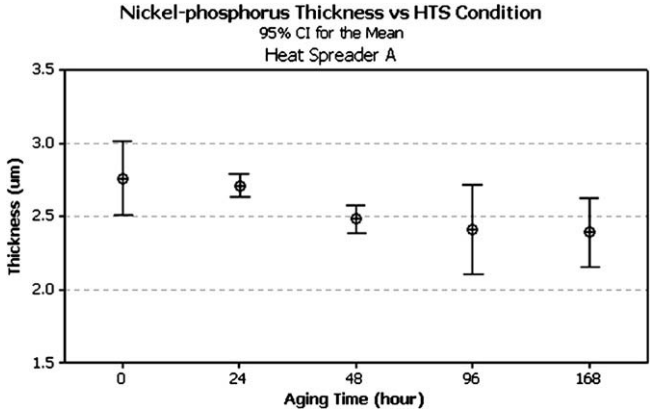

Fig. 6. Nickel–phosphorus thickness with different time conditions in heat spreader A.

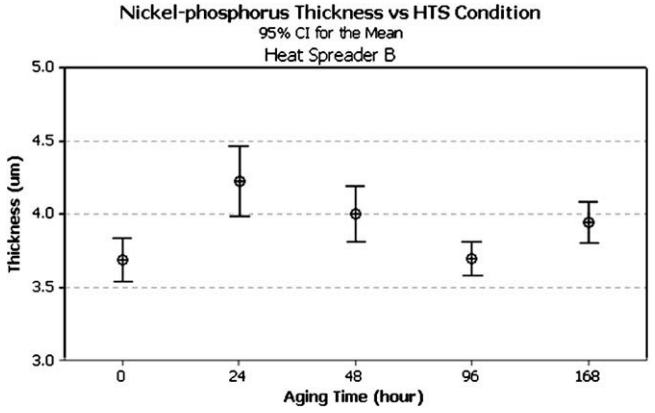

Fig. 7. Nickel–phosphorus thickness with different time conditions in heat spreader B.

Nano-flash thermal diffusivity meter in this section. Figs. 8 and 9 show the thermal diffusivity for heat spreaders A and B under different HTS condition. Comparing these two graphs, it clearly indicates that for all aging time, the thermal diffusivities as measured in mm^2/s are higher for heat spreader B than heat spreader A. Fig. 8 shows that the thermal diffusivity of heat spreader A is in the range of 35 mm^2/s to 60 mm^2/s, while Fig. 9 shows that the thermal diffusivity of heat spreader B is in the range of 60–85 mm^2/s. The lower thermal diffusivity of heat spreader A can be attributed to the presence of the nickel-and-copper alloys.

It is known that the thermal conductivity of an alloy of two metals is usually much lower than the thermal conductivity of both metals before they are alloyed. Even a small amount of foreign molecules with good heat conductivity in pure metal will seriously disrupt the transfer of heat in that metal. For example, the thermal conductivity of constantan (55%Cu, 45%Ni) is 23 W/mK, while the thermal conductivities of copper and nickel are 401 W/mK and 91 W/mK, respectively [3]. Fig. 10 shows the average thermal conductivity of the nickel–copper deposition layer inside heat spreader A under different aging hours. Thermal conductivities of nickel–copper deposition layer fall between 60 W/mK till 80 W/mK. This results show that the thermal conductivity of nickel–copper deposition layer is lower than both pure nickel and copper metal. This phenomenon is affecting thermal diffusivity because thermal diffusivity is proportional to thermal conductivity. Therefore, the Ni–Cu electrodeposition layer slows down the heat diffusing rate.

3.4. Effect of catalytic activation technique to surface roughness

The topographies of the heat spreader A and B were further analyzed using IFM. Two roughness parameters were used to determine the surface roughness of the heat spreaders, namely average roughness (R_a) and root-mean-square roughness (R_q). Average roughness is the average deviation of the profile form a mean line over the length of the assessment. Root-meat-square roughness is calculated by square rooting the mean of the profile deviation's square. Both heat spreaders' surface roughness calculated by two roughness parameter formulas are shown in Fig. 11. Roughness analysis using the IFM software quantitatively shows the difference of R_a between heat spreaders A and B which was 0.3074 μm and 0.5800 μm, respectively [18]. On the other hand, R_q of the heat spreaders A and B was 0.3889 μm and 0.7260 μm, respectively. The results in Fig. 11 show that heat spreader A with Ni–Cu electrodeposition layer has a much smoother surface than heat spreader B without Ni–Cu electrodeposition layer. The smoother surface of heat spreader A is due to the deposition of nickel–copper which has smoothened up the copper surface earlier. A rougher surface is more difficult for solid thermal interface material to fill up the crevices of the heat spreader and the effectiveness of heat dissipation is reduced. However, this effect can be minimized by using silicone gel thermal interface material which conforms better to surface irregularities [1].

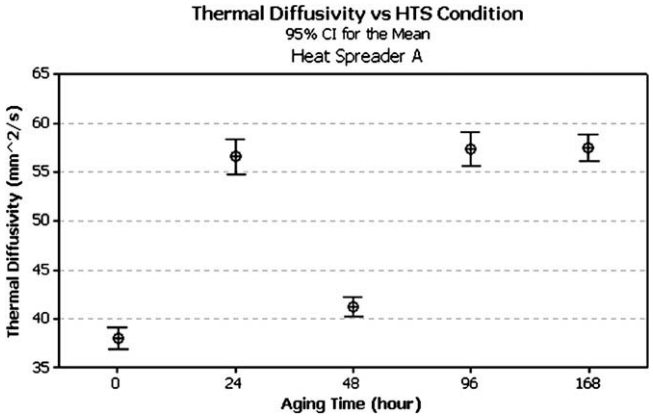

Fig. 8. Thermal diffusivity of heat spreader A at different time conditions.

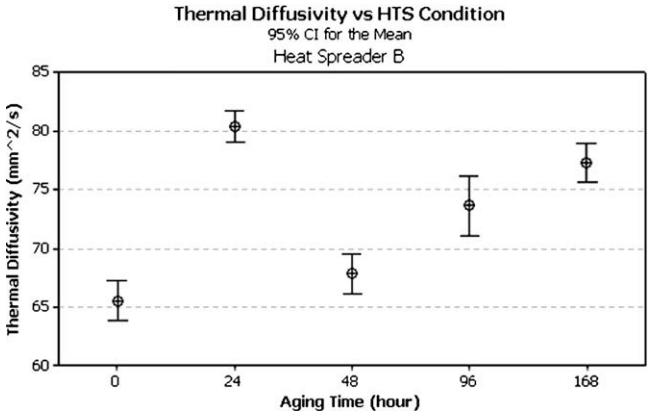

Fig. 9. Thermal diffusivity of heat spreader B at different time conditions.

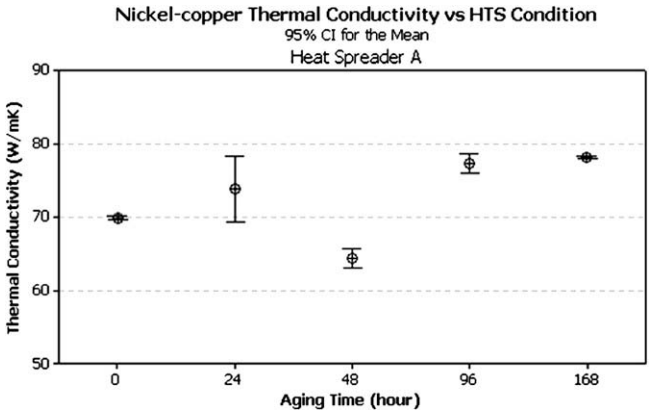

Fig. 10. Thermal conductivity of heat spreader A at different time conditions.

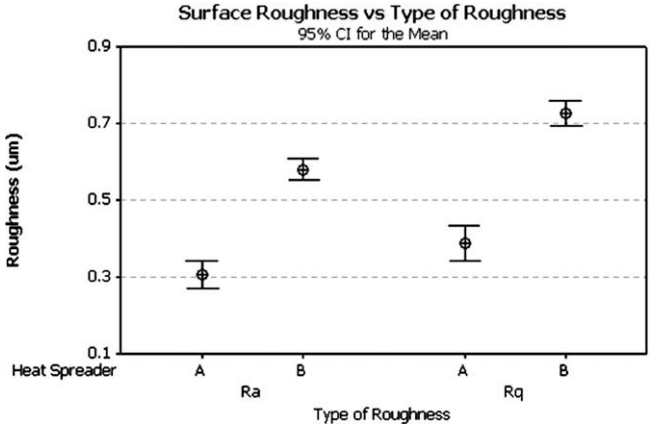

Fig. 11. Roughness of different heat spreaders under different roughness parameters.

4. Conclusion

This study shows that galvanic catalytic activation of heat spreaders before nickel plating significantly improves the thermal performance relative to thin copper strike activation because the galvanic initiation technique does not form any nickel–copper electrodeposition layer which has a low thermal conductivity. Even though galvanic initiation technique has a rougher surface, it can easily be resolved by using better thermal interface material. Therefore, it can be concluded that the galvanic initiation could be a better choice as this technique results in copper heat spreaders with higher thermal diffusivity.

Acknowledgements

The authors wish to acknowledge the Ministry of Science, Technology and Innovation (MOSTI), Malaysia under the IRPA Grant No. 03-02-02-0121 PR001 for financial supports. In addition, the authors would like to express their appreciation to the Science and Technology Faculty of the Universiti Kebangsaan Malaysia and the Freescale Semiconductor Malaysia Ltd., for their kind support in this work.

References

[1] Samson EC, Machiroutu SV, Chang JY, Santos I, Hermerding J, Dani A, et al. Interface material selection and a thermal management technique in second-generation platforms built on Intel Centrino mobile technology. Intel Technol J 2005;9(1):75–86.
[2] Prasher R. Thermal interface material: historical perspective, status, and future directions. Proc IEEE 2006;94:1571–86.
[3] Cengel YA. Heat and mass transfer: a practical approach. 3rd ed. Boston: McGraw-Hill; 2006.
[4] Yamada T, Yamamoto A, Fujiwara M, Kunigi Y. Strength evaluation and effect of graphite on strength of electroless nickel plating on cast iron. J Mater Sci 1993;28:3513–8.
[5] Chen Y, Cao M, Xu Q, Zhu J. Electroless nickel plating on silicon nanoparticles. Surf Coat Technol 2003;172:90–4.
[6] McKinnon HW. Nickel plating: industry practices control technology and environmental management. EPA United States Environmental Protection Agency; 2003.
[7] Cui G, Li N, Li D, Chi M. Study of optimized complexing agent for low-phosphorus electroless nickel plating bath. J Electrochem Soc 2005;152(10):C669–74.
[8] Watanabe H, Honma H. Direct electroless nickel plating on copper circuits using DMAB as a second reducing agent. In: 1998 IEMT/IMC Proceedings; 1998. p. 149–53.
[9] Aschenbrenner R, Ostmann A, Beutler U, Simon J, Reichl H. Electroless nickel/copper plating as a new bump metallization. IEEE Trans Compon Pack Manuf Technol – Part B 1995;18:2.
[10] Chen WP, Lu SG, Chan HLW. Influence of electroless nickel plating on I/V characteristics and its implications for reliability in ZnO-based ceramic varistors. Mater Sci Eng 2003;B99:70–3.
[11] Singh S, Ghosh SK, Basu S, Gupta M, Mishra P, Groverb AK. Structural and magnetic study of an electrodeposited Ni/Cu thin film by neutron reflectometry. Electrochem Solid-State Lett 2006;9(3):J5–8.
[12] Sartorelli ML, Schervenski AQ, Delatorre RG, Klauss P, Maliska AM, Pasa AA. Cu–Ni thin films electrodeposited on Si: composition and current efficiency. Phys Status Solid 2001;187(1):91–5.
[13] Kwon YS, An VV, Ilyin AP, Tikhonov DV. Properties of powders produced by electrical explosions of copper–nickel alloys wires. Mater Lett 2006;61:3247–50.
[14] Bakonyi I, Toth-Kadar E, Toth J, Becsei T, Tarnoczi T, Kamasa P. Magnetic and electrical transport properties of electrodeposited Ni–Cu alloys and $Ni_{81}Cu_{19}$/Cu multilayers. J Phys: Condens Mat 1999;11:963–73.
[15] Giouroudi I, Orfanidou C, Hristoforou E. Circumferentially oriented Ni cylindrical thin films for torque sensor applications. Sensors Actuat 2003;A106:179–82.
[16] Rao GR, Mishra BG, Sahu HR. Synthesis of CuO, Cu and CuNi alloy particles by solution combustion using carbohydrazide and N-tertiarybutoxy-carbonylpiperazine fuels. Mater Lett 2004;58:3523–7.
[17] Fritz T, Mokwa W, Schnakenberg U. Material characterisation of electroplated nickel structures for microsystem technology. Electrochim Acta 2001;47:55–60.
[18] Kanungo J, Pramanik C, Bandopadhyay S, Gangopadhyay U, Das L, Saha H, et al. Improved contacts on a porous silicon layer by electroless nickel plating and copper thickening. Semicond Sci Technol 2006;21:964–70.
[19] Wulff F, Breach C, Stephan D, Saraswati, Dittmer K. Characterization of intermetallic growth in copper and gold ball bonds on aluminum metallization. In: Proc 6th EPTC Singapore; 2004. p. 348–53.